# Morphological Evaluation of Cytoarchitectonics of Aortic Graft at the Biotechnological Stage with Analysis of Changes in Laser-Induced Fluorescence Spectra

**D. V. Subbotin[1], P. M. Larionov[1], D. S. Sergeevichev[1], O. A. Subbotina[1], G. S. Zaitsev[1], R. B. Novruzov[1], A. M. Orishich[2], A. N. Malov[2], N. A. Maslov[2], I. A. Rozhin[2], E. L .Lushnikova[3], and L. M. Nepomnyashih[3]**

Translated from *Kletochnye Tehnologii v Biologii i Medicine*, No. 4, pp. 191-196, December, 2009
Original article submitted June 25, 2009

We performed a fluorescent microscopic examination of human and animal aortic grafts at different stages of decellularization. Treatment of aortic grafts with trypsin/EDTA solution for 48 h leads to their complete decellularization and preserved the connective tissue fiber backbone, which gains a netlike structure. The use of this protocol of decellularization leads to disappearance of subintimal calcium deposits in human aortic grafts. Differences in laser-induced fluorescence spectra of aortas before decellularization and at different stages of this process were revealed. Our findings suggest that the use of fluorescence induced by excimer lasers is promising for identification of the composition of biological tissues, analysis of their state, and the presence of changes.

**Key Words:** *human and animal aortic grafts; decellularization; fluorescent microscopy; laser-induced fluorescence; excimer laser*

According to WHO data, cardiac pathology remains one of the main causes of disability and death all over the world. Dysfunction of valve structures is one of the main causes of high morbidity and mortality [2]. Until recently, replacement of affected structures with artificial valves was the only effective method of valve failure correction. However, long-term observations showed that creation of artificial valves from synthetic materials is fraught with various complications [10]. Xenovalves also have some drawbacks related to high risk of xenotransplant dysfunction due to peculiarities of the anatomy of the same heart portions in human and animals and high risk of immunological conflicts and transmission of unknown infections [6,7]. This problem can be solved by the development of tissue engineering technologies for creation of human valves [6-8,15]. However, for successful transplantation, the fragments including valves should have certain mechanic, hemodynamic, and resistance characteristics [5].

The development of technologies for the creation of new biocompetent organs and tissue fragments for transplantation was started more that 25 years ago. However, despite these bioengineering constructs demonstrated excellent hemodynamic and resistance characteristics in long-term animal experiments, they are not widely used [14,15]. These methods imply preparation of a 3D extracellular matrix not containing allogeneic cell elements [9,13] and creation of new

[1]E. N. Meshalkin Research Institute of Circulatory Pathology, Federal Agency for High-Technological Medical Care, Novosibirsk; [2]Institute of Theoretical and Applied Mechanics, Siberian Division of Russian Academy of Sciences; [3]Research Institute of Regional Pathology and Pathomorphology, Siberian Division of Russian Academy of Medical Sciences, Novosibirsk, Russia. ***Address for correspondence:*** patol@soramn.ru. P. M. Larionov

0007-4888/09/1484-0684 

basis cell strains for the formation of tissue or organ construct with subsequent reconstruction of extracellular matrix [6,10]; this allows prevention of certain complications

A promising trend is the development of rapid and precise diagnostics of the state of valve-containing aortic graft at the stage of decellularization on the basis of laser technologies [3,4,11,12].

The aim of the present study was to substantiate the use of laser-induced fluorescence (LIF) for identification of the composition of valve-containing fragment of the aorta and recording of its state and the presence of changes at biotechnological stages of the creation of the valve-containing graft.

## MATERIALS AND METHODS

The study was performed on 50 male rabbits aging 5-6 months (experimental material) and 50 fragments of the aorta (autopsy material). Valve-containing fragments of human aorta were obtained within the first 12-14 h after non-violent death (Novosibirsk Regional Bureau of Forensic Medical Examination). During autopsy, standard dissection of the aorta with aortic valve was performed according to standards and protocols of European Tissue Bank. The procedure of isolation, transportation, sterilization, cryopreservaton, and elimination of cell material from the structure of extracellular matrix of the valve-containing aortic fragment was developed.

The process of removal of the nuclear material consisted in elimination of autological cells with preservation of the structural organization of the extracellular matrix. After dissection, aortic fragments without adventitia under sterile conditions of a biosafety laminar box were incubated in a decellularizing trypsin–EDTA solution (0.5% trypsin and 0.02% EDTA) for 1 day at 37°C and with constant stirring. LIF was measured in native aortic samples (control, 1 h after autopsy and transportation in cold saline) and in decellularized fragments. Aortic grafts 1 h after autopsy and transportation in cold physiological saline served as the control. LIF was induced by krypton-fluorine (Kr-F) excimer laser (Institute of Theoretical and Applied Mechanics, Siberian Division of Russian Academy of Sciences) with λ=248 nm and pulse energy 5-10 mJ (5 msec exposure, $2\times10^6$ W pulse power).

Morphological examination of aortas at different stages of decellularization was performed: 2.5, 8, 24, and 48 h after the start of cell elimination (stages I, II, III, and IV, respectively). To this end, 7-μ sections were prepared on Microm HM-550 (Carl Zeiss), stained with fluorescent probes ethidium bromide (filter set No. 14, BP 510-560 nm, FT580, LP 590 nm), propidium iodide, and chlortetracycline (filter set No. 05, BP 395-440 nm, FT460, LP 470 nm). The studies were performed on Axioskop FL-40 microscope (AxioCam MRc camera, AxioVision 3.1 software).

Microstructure and chemical composition of valve-containing aortic fragments during decellularization were studied by the method of local analysis using scanning electron microscopy (SEM). Survey examination and X-ray structural analysis of aortic fragments were performed on a LEO1430VP scanning electron microscope with an OXFORD energy-dispersion spectrometer for X-ray analysis. A D8 GADDS X-ray diffractometer (Bruker) was also used. The results of microprobe analysis were quantitatively processes using INKA software.

The results of morphometric studies were processes by methods of variation statistics using Fisher–Student test [1].

## RESULTS

**Fluorescent microscopy of aortic grafts at different stages of cellularization.** Fluorescent probe assay provides information on the processes occurring in the tissue during preparation of the aortic graft and on the degree of degradation of the tissue and nuclear material, it also allows identifying the factors inducing shifts in LIF spectra and evaluating method efficiency.

Survey fluorescent microscopy of preparations stained with ethidium-bromide (200 preparations of rabbit aortas from 40 animals) and propidium iodide (150 preparations from 30 human aortas) revealed similar tissue transformation of aortic fragments at the stages of biotechnological processing: gradual decrease and complete disappearance of nucleus-containing cells in the aortic walls at different stages of decellularization, followed by loosening and progressive edema of the aortic wall (Fig. 1, *a*), disappearance of extracellular matrix with the formation of a fibrous netlike structure (Fig. 1, *b*).

Subsequent fluorometry of rabbit aortic fragments demonstrated the ethidium bromide incorporation dynamics. Bearing in mind that ethidium bromide binds to DNA fragmentation sites, the total fluorescence of this probe reflects the degree of DNA degradation in the aortic graft during decellularization process. We observed a significant decrease ($p<0.05$) in total fluorescence intensity of ethidium bromide in aortic samples at two last stages of decellularization (after 24 and 48 h) compared to the initial fluorescence of the native preparation and preceding biotechnological stages (2.5 and 8 h, Fig. 2, *a*). Reduced incorporation of ethidium bromide intercalating into DNA at two last stages of biotechnological processing of rabbit aortic grafts and aortic homografts attests to elimination of nucleus-containing material.

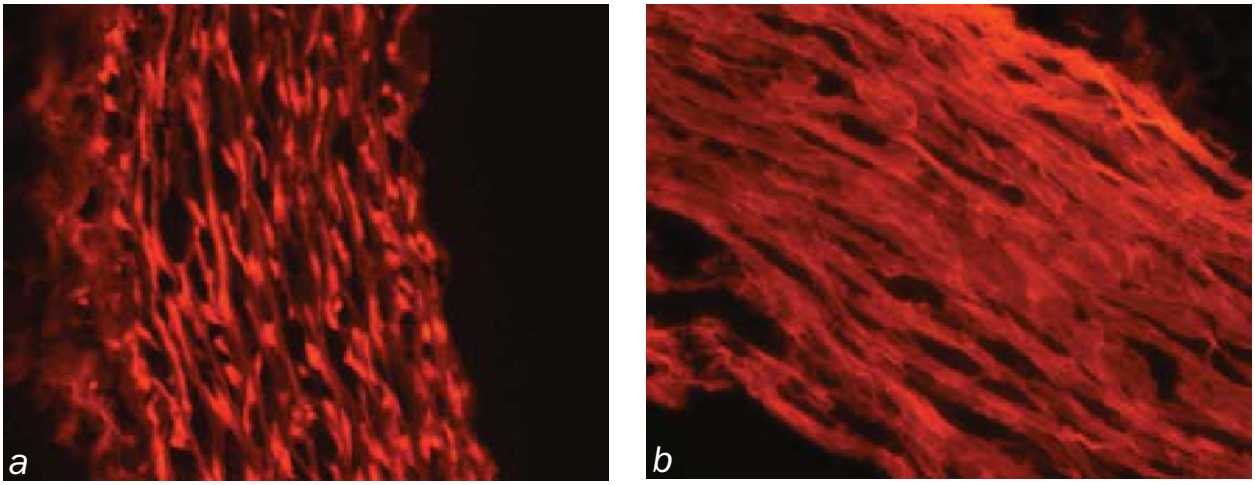


**Fig. 1.** Fluorescent microscopy of rabbit aortic grafts at different stages of decellularization. Ethidium bromide staining (×260). *a*) the presence of nucleated cells, moderate intercellular edema 2.5 h after the start of decellularization; *b*) complete absence of nucleated cells, fiber swelling after 48 h.

The dynamics of fluorescence of chlortetracycline probe was studied in the human aortic wall at the stage of biotechnological processing of acellular graft. Aortic samples before decellularization were characterized by diffuse fluorescence in interfibrillar spaces against the background of elastic fiber contouring (Fig. 3, *a*), while at the last stage of biotechnological processing of the acellular graft, the intensity of fluorescence decreased, fiber contouring being preserved (Fig. 3, *b*). Incorporation of chlortetracycline into aortic samples significantly decreased at all stages of decellularization (Fig. 2, *b*) compared to the control ($p<0.05$). The significant decrease in fluorescence intensity at stages 3 and 4 of decellularization compared to the initial stage ($p<0.05$) reflects gradual loss of nuclear material (decellularization) by aortic homografts and a decrease in total calcium content (decalcination).

Survey scanning microscopy in the back-scatter mode revealed longitudinally-oriented linear intermittent calcium deposits in the subendothelial layer of native aortic grafts (Fig. 4, *a*). Focal deposits (1-10 μ) were also found in the subendothelial layer. Linear intermittent calcium deposits were present in all samples, while focal deposits were found in 50% samples. X-ray spectral analysis of calcium/phosphorus ratio showed that these deposits are presented by apatites.

After decellularization, a monomorphous picture without linear intermittent deposits was observed (after 24 and 48 h). The aortic grafts lost both the extra- and intracellular calcium. Survey scanning microscopy revealed transformation of aortic wall at the final stages of decellularization: slip of individual fibers, disturbances in regular pattern of fiber

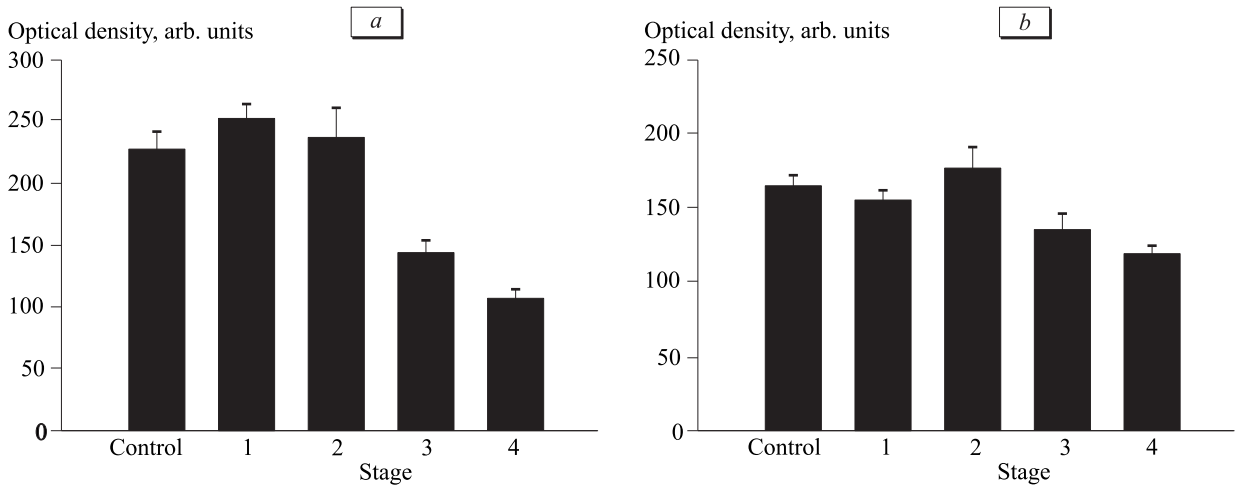


**Fig. 2.** Changes in fluorescence intensity of aortic grafts during decellularization. *a*) fluorometry of rabbit aorta after ethidium bromide staining; *b*) fluorometry of human aorta after chlortetracycline staining. Abscissa: stages of decellularization.

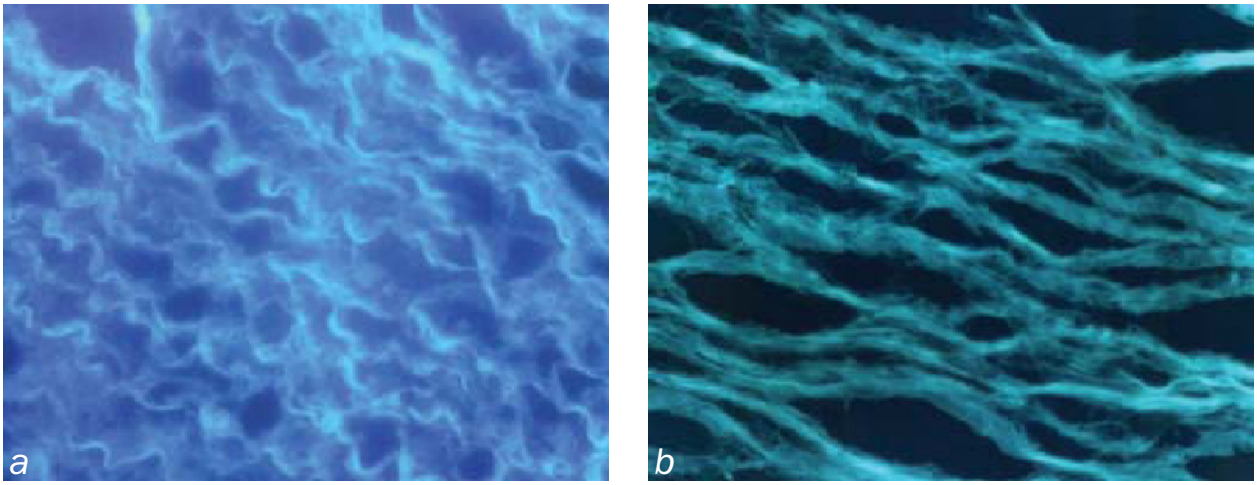


**Fig. 3.** Fluorescent microscopy of human aortic grafts at different stages of decellularization. Chlortetracycline staining (×260). *a*) native aorta, high fluorescence intensity in intercellular spaces against the background of fiber contouring; *b*) complete absence of visible fluorescence in interfibrillar spaces and preserved fiber contouring after decellularization.

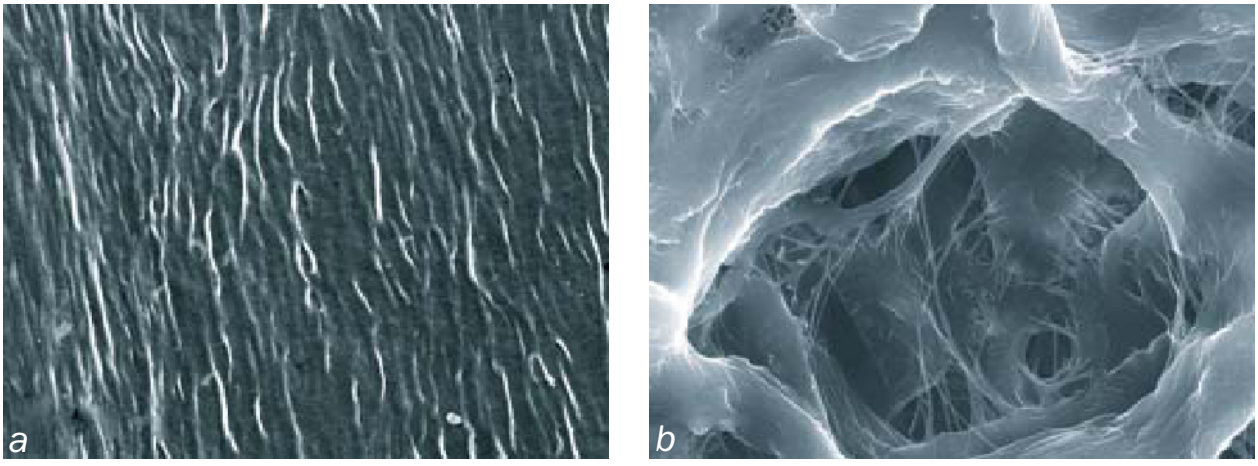


**Fig. 4.** Electron microscopy of aortic grafts before and after decellularization. *a*) linear intermittent deposits on the surface of aortic homografts before and after decellularization. SEM in the electron back-scatter mode (×1300); *b*) formation of a netlike structure with cell diameter of 40-50 μ of an aortic homograft after decellularization. Survey SEM ×13,000).

organization in the aortic wall, appearance of netlike structures (Fig. 4, *b*), which was not typical of native aortic samples.

**Evaluation of LIF spectra of human valve-containing aortic grafts during decellularization.** Noncoincident LIF spectra of different native aortas and considerable differences between the proximal and distal ends of the same aorta are presented on Figure 5, *a*. Differently directed changes in LIF spectra of aortas were detected 2.5 h after the start of decellularization (Fig. 5, *b*). The intensity of some LIF spectrum bands of the first aortic segment tended to increase, while in the second aortic segment, a tendency towards a decrease in fluorescence intensity at 380-520 nm was noted. At the final step of decellularization, LIF intensity decreased and the second peak at 380-520 nm disappeared (Fig. 5, *c*).

Despite the initial differences in LIF spectra of aortas obtained after autopsy, biotechnological processing for the creation of acellular graft led to disappearance of the peak at 420-570 nm, which was a result of decalcification and elimination of nuclear material.

Thus, treatment of aortic grafts with trypsin–EDTA solution for 48 h leads to their complete decellularization and preserved the connective tissue fiber backbone, which gains a netlike structure. The use of this protocol of decellularization leads to disappearance of subintimal calcium deposits in the aortic grafts. Evaluation of LIF spectra of aortas revealed their differences before and at different stages of decellularization. These data suggest that UV laser (λ=248 nm) can be successfully used for the diagnostic of the state of biological tissues, *e.g.* for evaluation of the degree of decellularization of valve-containing aortic grafts.

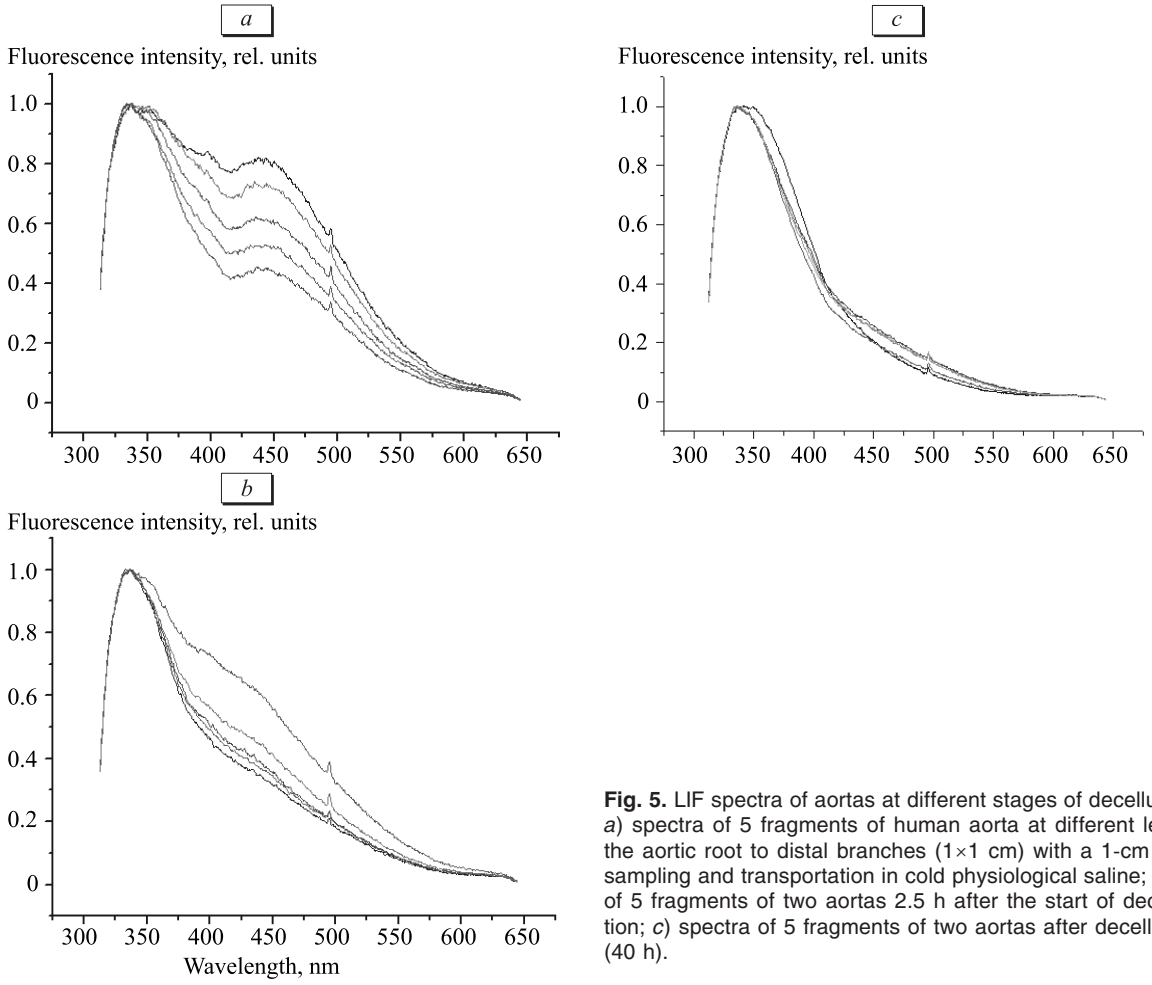


**Fig. 5.** LIF spectra of aortas at different stages of decellularization. *a*) spectra of 5 fragments of human aorta at different levels from the aortic root to distal branches (1×1 cm) with a 1-cm step after sampling and transportation in cold physiological saline; *b*) spectra of 5 fragments of two aortas 2.5 h after the start of decellularization; *c*) spectra of 5 fragments of two aortas after decellularization (40 h).

## REFERENCES

1. G. G. Avtandilov, *Morphometry in Pathology* [in Russian] Moscow (1973).
2. L. V. Kakturskii, *Sudden Cardiac Death (Clinical Morphology)* [in Russian], Moscow (2001).
3. P. M. Larionov, A. N. Malov, N. A. Maslov, and A. M. Orishich, *Zh. Prikladn. Spektroskop.*, **66**, No. 6, 846-849 (1999).
4. P. M. Larionov, A. M. Orishich, A. N. Malov, and N. A. Maslov, *Opt. Atmosf. Okeana*, **13**, No. 3, 305-308 (2000).
5. F. D. Affonso da Costa, P. M. Dohmen, S. V, Lopes, *et al.*, *Artif. Organs*, **28**, No. 4, 366-370 (2004).
6. A. Bader, T. Schilling, O. E. Teebken, *et al., Eur. J. Cardiothorac. Surg.*, **14**, No. 3, 279-284 (1998).
7. S. Cebotari, H. Mertsching, K. Kallenbach, *et al., Circulation*, **106**, No. 2, Suppl. I, I63-I68 (2002).
8. R. C. Elkins, P. E. Dawson, S. Goldstein, *et al., Ann. Thorac. Surg.*, **71**, No. 5, Suppl., S428-S432 (2001).
9. Grauss R.W., M.G. Hazekamp, Oppenhuizen F. *et al., Eur. J. Cardiothorac. Surg.*, **27**, No. 4, 566-571 (2005).
10. S. P. Hoerstrup, R. Sodian, S. Daebritz, *et al., Circulation*, **102**, No. 19, Suppl. 3, III44-III49 (2000).
11. P. M. Larionov, A. V. Kushnir, *et al., Proceed. SPIE*. **4900**, 1039-1044 (2002).
12. P. M. Larionov, A. N. Malov, N. A. Maslov, *et al., App. Optics.*, **39**, No. 22, 4031-4036 (2000).
13. W. Li, W.-Y. Liu, D.-H. Yi, *et al., Asian Cardiovasc. Thorac. Ann.,* **15**, No. 2, 91-96 (2007).
14. M. F. O'Brien, S. Goldstein, S. Walsh, *et al., Semin. Thorac. Cardiovasc. Surg.,* **11**, No. 4, Suppl. 1, 194-200 (1999).
15. T. Shinoka, D. Shum-Tim, P. X. Ma, *et al., J. Thorac. Cardiovasc. Surg.*, **115**, No. 3, 536-545 (1998).